IMEKO 22nd TC3, 12th TC5 and 3rd TC22 International Conferences
3 to 5 February, 2014, Cape Town, Republic of South Africa

MATHEMATICAL MODEL OF CHECKWEIGHER WITH ELECTROMAGNETIC FORCE COMPENSATION (2ND REPORT)

Y. Yamakawa/Presenter, and T. Yamazaki

Univ. of Tokyo, Tokyo, Japan, Yuji_Yamakawa@ipc.i.u-tokyo.ac.jp
Oyama National College of Technology, Tochigi, Japan, yama@oyama-ct.ac.jp

Abstract: In this research we discuss behaviors of a high speed mass measurement system with conveyor belt (a checkweigher). The objective of this paper is a proposal of a simple dynamic model of the system. The dynamics of the checkweigher with Electro-Magnetic Force Compensation (simply called EMFC) can be approximated by a mass-spring-damper system as a physical model, and an equation of motion is derived. Model parameters can be estimated from the experimental data. Then, comparisons of the simulation results with the realistic responses are carried out. Finally, effects of floor vibration on the mass measurement system will be explored. The dynamic model obtained offers practical and useful information to implement control scheme.

Keywords: mass measurement, electromagnetic force compensation system, dynamic behavior, floor vibration.

1. INTRODUCTION

In recently, a high-accuracy and high-speed mass measurement system of packages moving the conveyor belt operated at high speed, so-called the checkweigher, has been getting more important in the food and logistics industries etc. To achieve the high-speed (continuous) measurement, packages should be moved in sequence. It means that the measuring time for one package is very short. In the near future, the continuous mass measurement for 300 products per minute will be required.

In general, there exist two types of the measurement system of the checkweigher, such as a load cell type [1-4] and an electromagnetic force compensation (EMFC) type. In this research, we adopt the EMFC type in order to achieve the high-speed and high-accuracy mass measurement.

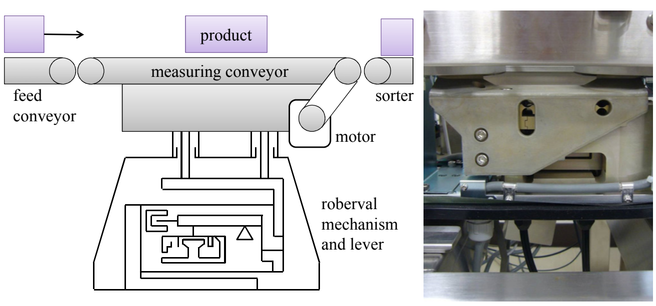

(a) Measurement system (b) Roberval mechanism

Fig. 1. Photographs of checkweigher

Until now, the dynamic behavior of the EMFC system has not still been suggested. Our final goal is that the performance of the checkweigher can be improved for high-speed and high-accuracy. To do this, it is significantly necessary to develop a control scheme of the EMFC based on the dynamic model. Thus, we propose a simple dynamic model of the checkweigher with EMFC [5]. In this paper, we describe the simple dynamic model of the system, and estimate model parameters of the system. Then we confirm the validity of the proposed model for various situations such as step responses for an open-loop system and a closed-loop system, and frequency responses about effect of floor vibrations.

2. MEASUREMENT SYSTEM

Fig. 1(a) shows the figure of the checkweigher. The feed conveyor is located in the left of the measuring conveyor and the sorter is located in the right. The products are moved by the feed conveyor, the mass of product measured by measuring conveyor and the product out of the measurable range is removed by a sorter.

The enlarged photograph of the mass measurement mechanism in the checkweigher is shown in Fig. 1(b). The mass measurement system consists of weighing platform, the Roberval mechanism, the lever linked Roberval mechanism, the counter weight, the electromagnetic force actuator and the displacement sensor. By applying the Roberval mechanism to the measurement mechanism, the mass of the product can be measured even if the product locates in everywhere over the weighing platform.

The mass of the product is estimated from the current of the electromagnetic force actuator to control the lever displacement.

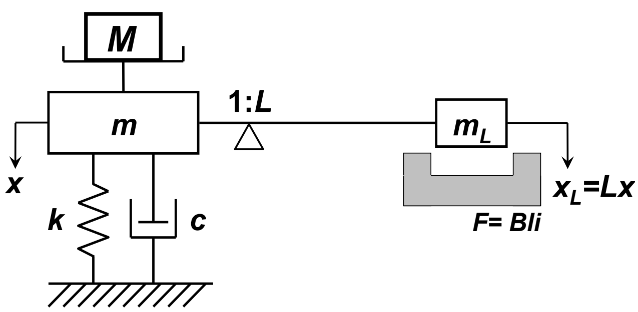

Fig. 2. Physical model of measurement system

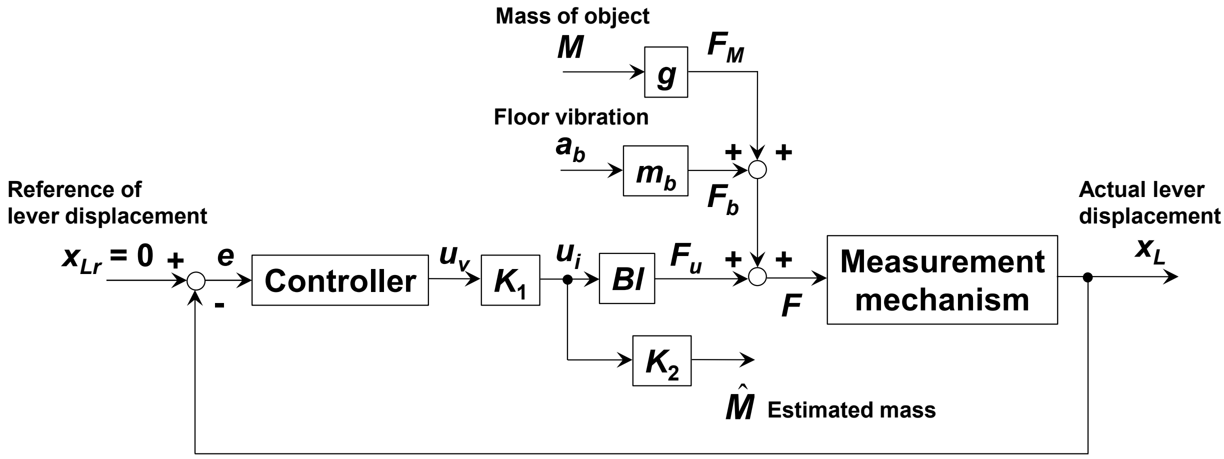

Fig. 3 Block diagram of measurement system

The measuring method of mass can be explained as follows:

1. When the product of the mass M is put on the measurement system, the displacement of the Roberval mechanism is caused.
2. The displacement of the Roberval mechanism is magnified twenty times by the lever.
3. The magnified displacement can be measured by the displacement sensor.
4. The current is controlled so that the displacement of the lever can be maintained at zero.
5. The current is measured and the current is converted to the estimated mass by using the linear function.

3. MODELING

Fig. 2 shows a physical model of the measurement system. An equation of motion about mass m can be given by:

$$(M + m + m_L L^2)\ddot{x} + c\dot{x} + kx = Mg + FL \quad , \qquad (1)$$

where m is mass of the Roberval mechanism, M mass of an product to be measured, c a damping coefficient, k a spring constant, g (= 9.8 m/s^2) the acceleration of gravity, L (= 20 m/m) the lever ratio, and x the displacement of mass m. And, m_L mass of the lever, x_L (= $-Lx$) the displacement of the lever, and F (= Bli, where B is a density of magnetic flux, l a length of the coil, and i a current.) an electromagnetic force which means the control input in order to control the position x_L of the lever.

From equation (1), the natural frequency f can be described by

$$f = \frac{1}{2\pi}\sqrt{\frac{k}{M + m + m_L L^2}} \quad . \qquad (2)$$

From the experimental result, the natural frequency f of the system is 5 Hz and the damping ratio is 0.08. Thus, the spring constant k can be calculated as follows:

$$k = (2\pi f)^2 \times (M + m + m_L L^2) = 89.2 \times 10^3 \quad . \qquad (3)$$

The damper coefficient can be adjusted so as to match the convergence rate in the responses of the lever.

From Eq. (1), the Roverbal displacement at steady-state for the open-loop system (F = 0) can be described by:

$$x = \frac{Mg}{k} \, . \qquad (4)$$

In addition, the lever displacement at steady state, that is magnified the Roverbal displacement by the lever, can be obtained by the following equation.

$$x_L = -Lx \, . \qquad (5)$$

The simulation of the measurement system can be performed by using Eqs. (1)-(5). Fig. 3 shows a block diagram of measurement system. In simulations and experiments, the validity of the model can be confirmed by comparing between the sensor outputs of the lever displacement (x_L).

4. EXPERIMENTAL AND SIMULATION RESULTS

In this section, the validity of the proposed model is confirmed with comparisons between simulation result and experimental results for the open-loop system, the close-loop system. In particular, we discuss effect of floor vibrations as disturbances in usage environment.

Open-loop response: The validity of the proposed model is examined with comparisons between the simulation result and the experimental result for the open-loop system.

Fig. 4 depicts experimental and simulation results for M = 0.01, 0.02, 0.05 and 0.1 kg. The red line and the blue line mean the experimental result and the simulation result, respectively. The start-up operation is the time when the product of the mass M is put on the measurement system. Then, when the time is 0.2 s, the product of the mass M is removed. At the same time, the lever displacement x_L is measured by the displacement sensor. In Fig. 4, the vertical axis shows the displacement sensor output of the lever displacement.

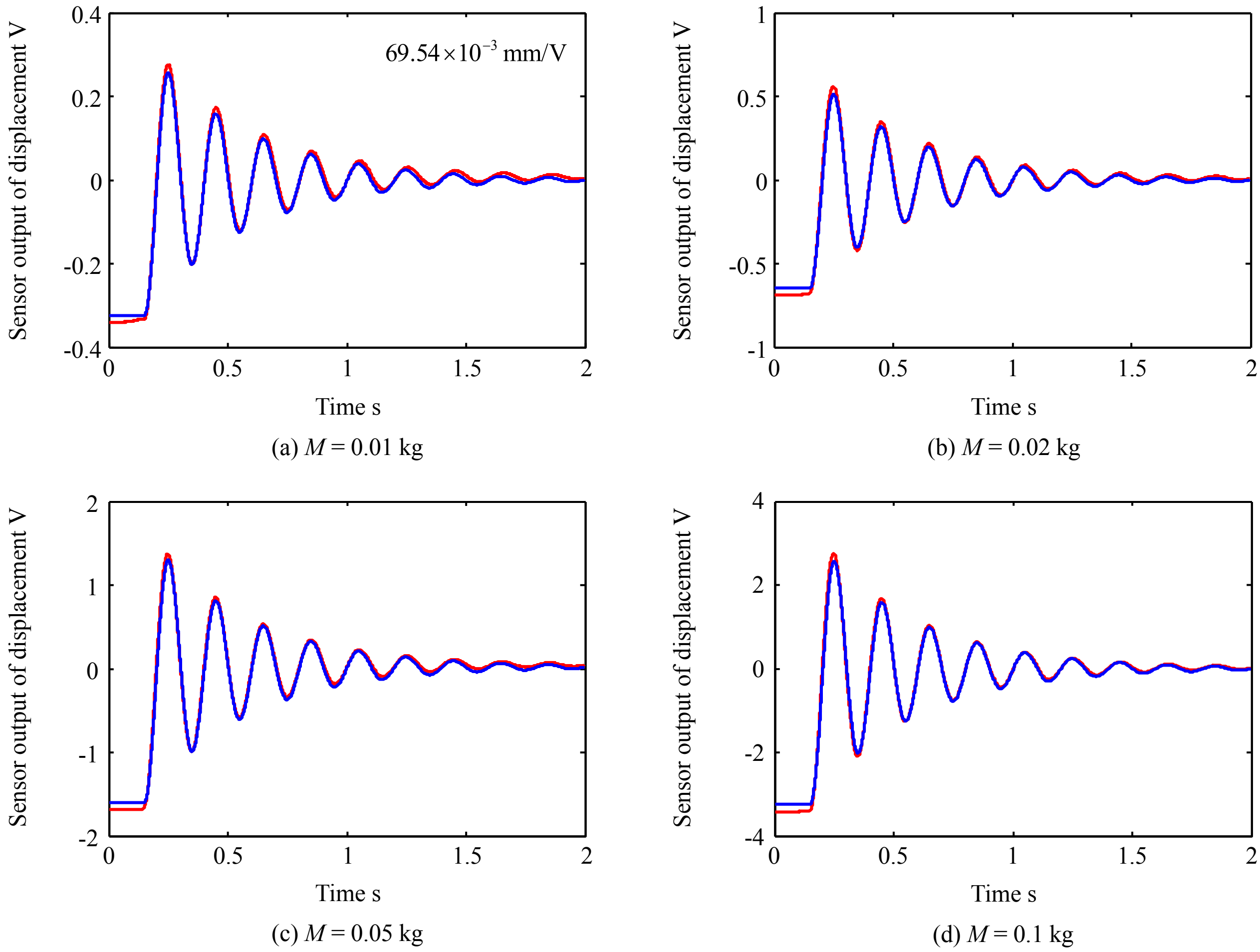

Fig. 4 Comparisons between experimental results and simulation results (closed-loop)

It can be seen from these figures that the responses of the simulation made a good agreement with the experimental results perfectly. Thus, the validity of the proposed model is confirmed for the open-loop system.

Closed-loop response: Here we explain comparison of the experimental with simulation results for a close-loop system. The electromagnetic force is controlled by PID control scheme. Taking the actual circuit of the D action into account, the ideal D action cannot be implemented. So, we use an approximated D action. Thus, the transfer function of the PID controller $C(s)$ can be described by,

$$C(s) = k_p + \frac{k_i}{s} + \frac{k_{dn} s}{k_{dd} s + 1} \tag{6}$$

where k_p is the proportional gain. k_i is the integral gain. k_{dn} and k_{dd} are the numerator and denominator coefficients of the differential gains, respectively. And, the control voltage $U_v(s)$ (Laplace transform of $u_v(t)$) can be adjusted as follows.

$$U_v(s) = C(s)E(s) \tag{7}$$

where $E(s)$ is Laplace transform of $e(t)$ and $e(t)$ ($= x_{Lr} - x_L$) is the error between the reference x_{Lr} and the displacement sensor output of the lever x_L. The PID control can be performed by FPGA at every 0.1 ms.

Fig. 5 depicts experimental and simulation results for M = 0.01, 0.02, 0.05 and 0.1 kg. The red line and the blue line mean the experimental result and the simulation result, respectively. The simulation and experimental conditions are the same as the open-loop system.

The response such as the convergence time, the rise time and the settling time between the simulation and experimental results are almost the same. Thus, the validity of the proposed EMFC model is confirmed. We consider that the reasons of modeling error are the friction force in small displacement and the magnification mechanism of the lever. However, a peak value of the simulation result for M = 0.1 kg is different on that of the experimental result. Moreover, the high-frequency response occurs in the experiments due to system noises.

Responses to floor vibrations: Here we explore effect of floor vibrations to the mass measurement system. And we also discuss the validity of the proposed model for dynamical characteristics. Simulations and experiments are carried out in the closed-loop system. In case of the floor vibration in the open-loop system, the saturation of the lever displacement x_L occurs due to the mechanical limitation to avoid the system breakdown. As a result, the comparison of the experiments with the simulations in the open-loop system cannot be performed.

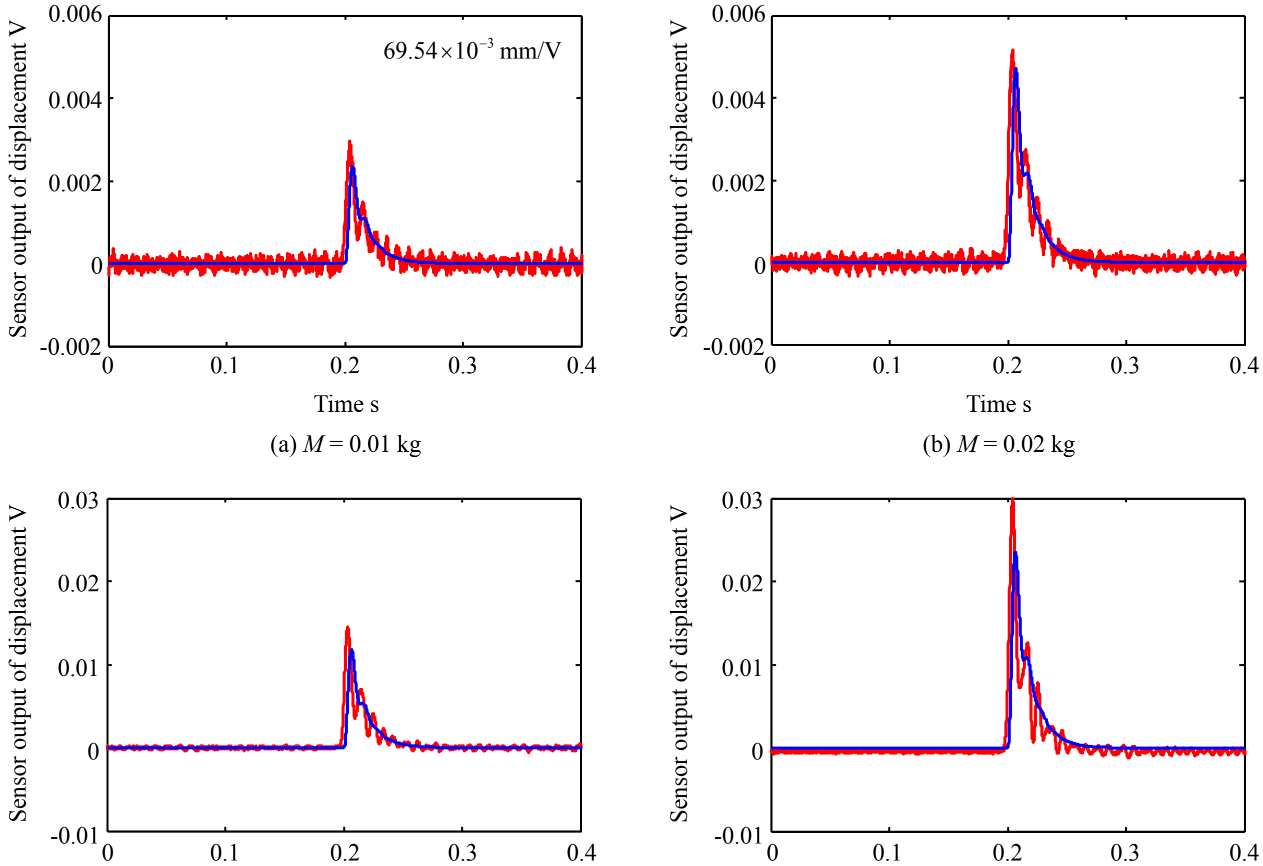

(a) $M = 0.01$ kg (b) $M = 0.02$ kg (c) $M = 0.05$ kg (d) $M = 0.1$ kg

Fig. 5 Comparisons between experimental results and simulation results (closed-loop)

In experiments, the floor vibrations are acted on the system by using a vibrator. In simulations, floor vibration inputs are applied to the system as the environmental disturbance, as shown in Fig. 3. And, displacement of the floor vibrations in the simulations can be given by

$$x_b(t) = A \sin \omega t \quad , \tag{8}$$

where $x_b(t)$ is the displacement of floor vibration, A [mm] is an amplitude of the floor vibration, ω [rad/s] (= $2\pi f$, f is a frequency) is an angular frequency of the floor vibration, and t is the time. Therefore an acceleration $a_b(t)$ of the floor vibration can be described as follows:

$$a_b(t) = -A\omega^2 \sin \omega t \quad . \tag{9}$$

And an input of floor vibration to the system can be obtained by multiplier of the acceleration $a_b(t)$ and the mass m_b of the part of the Roverbal mechanism.

Fig. 6 shows experimental results and simulation results for the floor vibrations. The conditions about the floor vibration for experiments and simulations in Fig. 6(a), (b) and (c) are the followings:

(a) A = 1 mm, f = 10 Hz
(b) A = 1 mm, f = 5 Hz
(c) A = 1.25 mm, f = 5 Hz

In Fig. 6, the vertical axis shows an estimated mass of the system.

As can be seen from Fig. 6, same responses about the amplitude and the frequency results in the experiment and the simulation can be obtained. Consequently, we can examine the effect of floor vibrations using the proposed model. In general, the frequency of the floor vibration can be considered to be range from 1 to 3 Hz. Thus, the actual floor vibration can be evaluated using the proposed model.

5. CONCLUSIONS

In this paper, we proposed a dynamic model of the measurement system with Electro-Manetic Force Compensation (EMFC). The dynamic model was approximated by a mass-spring-damper system. Then we estimated the model parameters (c: the damping coefficient, k: the spring constant) using the experimental data. Then, the validations of the proposed model for the open-loop system and the closed-loop system were confirmed. In addition, we explored the effect of the floor vibrations (disturbance of dynamical usage environment) and verified that the effect of the floor vibration can be duplicated by the proposed dynamic model. As a result, we can simulate dynamic behaviors of the mass measurement system for various situations by using the proposed model.

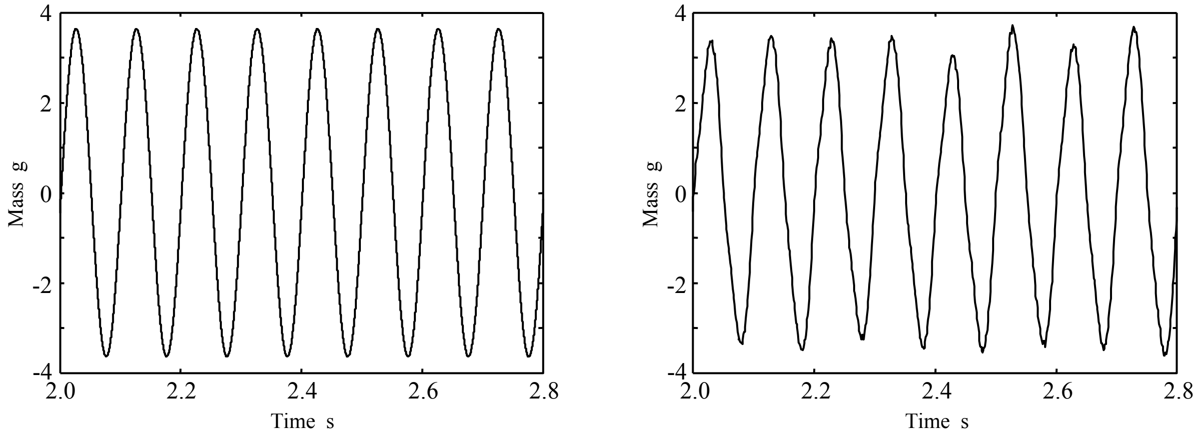

(a) $A = 1$ mm, $f = 10$ Hz

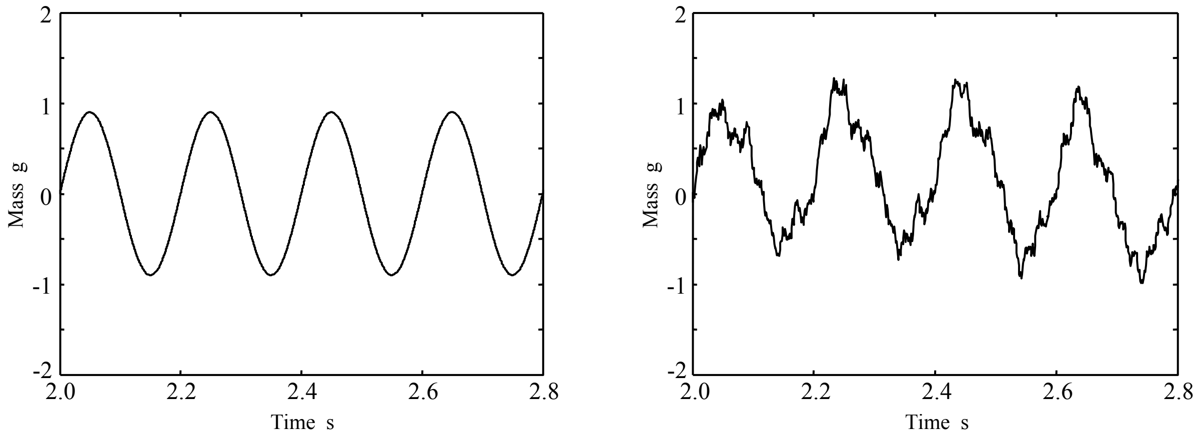

(b) $A = 1$ mm, $f = 5$ Hz

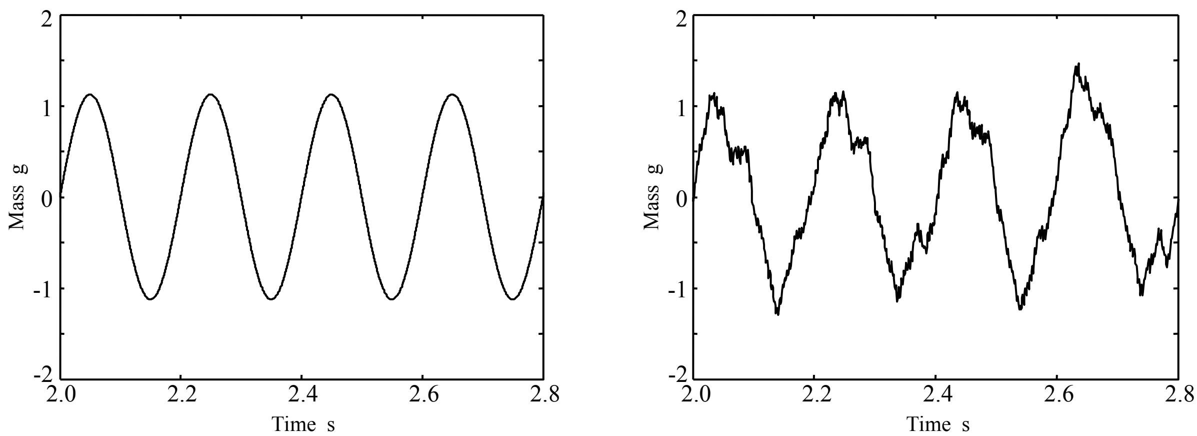

(c) $A = 1.25$ mm, $f = 5$ Hz

Fig. 6 Comparisons between experimental results and simulations result about floor vibrations

In the future, we will design a new control system of the mass measurement system using the proposed model in order to improve the accuracy of the mass measurement and the convergence time for the working efficiency.

6. REFERENCES

[1] Ono T., "Basic point of dynamic mass measurement", Proc. SICE, pp. 43-44, 1999.

[2] Ono T., "Dynamic weighing of mass", Instrumentation and Automation 12, No. 2, pp. 35, 1984.

[3] Lee W.G. et al., "Development of speed and accuracy for mass measurements in checkweighers and conveyor belt scales", Proc. ISMFM, pp. 23-28, 1994.

[4] Kameoka K. et al., "Signal processing for checkweigher", Proc. APMF, pp. 122-128, 1996.

[5] Y. Yamakawa and T. Yamazaki, Mathematical Model Of Checkweigher With Electromagnetic Force Compensation, Proc. XX IMEKO World Congress, pp. 208–211, 2012.